IGM83-138-096
Etude No. 96
Projet 8351-138

A METHOD OF COMPUTATION OF THE PRESSURE EFFECT ON MELT VISCOSITY

by

L.A. Utracki
National Research Council of Canada
Industrial Materials Research Institute
75 De Mortagne Blvd., Boucherville, Quebec J4B 6Y4

Presented at the third NRCC-IMRI Mini-symposium
"Modeling-'84"
January 24, 1984

CNRC 22983

A METHOD OF COMPUTATION OF THE PRESSURE EFFECT ON MELT VISCOSITY

by

L.A. Utracki

National Research Council Canada
Industrial Materials Research Institute
75 De Mortagne Blvd., Boucherville, Quebec, Canada, J4B 6Y4

ABSTRACT

Simha's equation of state provides the relation between reduced pressure, temperature and volume ($\tilde{P}$, $\tilde{T}$ and $\tilde{V}$, respectively) and the occupied site fraction, $y = y(\tilde{P}, \tilde{T})$. The latter theoretical parameter combines the P and T effects on the occupied and unoccupied ("free volume") part of the model liquid. It can be computed for each liquid once the thermodynamic reducing parameters are known. Empirical correlation between published zero shear viscosity data, $\eta = \eta(P, T)$, and y indicates that for n-paraffins and molten polymers η is a single parameter function: $\eta = \eta(y)$. The mathematical form of this dependence was explicitly given for n-paraffins. However, for polymers the correlation depends on molecular weight, molecular weight distribution, branching, composition, etc. In practical terms, $\eta = \eta(y)$ should be determined for each polymer by measuring the temperature dependence of η in as wide a range of T as possible. The pressure effect on η can be determined from $\eta = \eta(y)$ plot, knowing the $y = y(\tilde{P}, \tilde{T})$ relation.

INTRODUCTION

The mathematical modeling of plastics processing involves iterative multi-variable computations (1-3). The inherent complexity of the method as well as the scarcity of rheological data leads to gross oversimplification of the polymer flow properties. Even now there are models incorporating the zero-shear viscosity, η, as the single rheological parameter. In the more sophisticated ones, the rate-of-shear, $\dot{\gamma}$, and the temperature, T, dependencies of viscosity, η, are introduced via the "power law" and Arrhenius equations respectively:

$$\ln \eta_{\dot{\gamma}} = \ln \eta(\dot{\gamma}=1) - (1 - n) \ln \dot{\gamma} \qquad (1)$$

$$(\partial \ln \eta)/\partial(1/T) \mid_{P=0} = E_a/R \qquad (2)$$

Only in the most advanced models of injection molding, is the pressure, P, effect also incorporated using the Cogswell simplification (4):

$$(\partial \ln \eta/\partial P)_T = - K(T)E_a \ . \qquad (3)$$

The temperature dependent K has to be determined experimentally for each polymer.

There are questions as to the extend of the pressure effect and the size of the error should it be neglected it. The demand for a better product, the need for faster production and resulting advances in processing equipment continuously increase the operating pressures. In extrusions and injection molding, the pressures are up to 50 and 700 MPa respectively. How much these pressures influence η_o depends on the relative temperature. Since P increases both the melting point, T_m, and the glass transition temperature, T_g, the effect can be truly dramatic (4-6); a thousand-fold increase in η_o for polystyrene, PS, was reported increasing P from 0.1 to 100 MPa.

HISTORICAL DEVELOPMENT

During the last few years, an effort has been made to seek the general form of η-behaviour of polymeric and non-polymeric liquids as functions of T and P (6-12). The work has been based on the free volume approach.

The isobaric T-effect has been successfully discussed on the basis of the Doolittle equation:

$$\ln\eta = A_o + B_o Y_D \tag{4}$$

where

$$Y_D = [(V-V_o)/V_o]^{-1} ,$$

A_o and B_o are equation constants, while V and V_o are molar or specific volumes at T and at T = 0(K), respectively. The V and V_o can be computed from the semi-empirical relation (13):

$$\ln \tilde{V} = S_o + S_1 \tilde{T}^{3/2} \tag{5}$$

where S_o and S_1 are parameters and symbols with the tilde indicating the reduced variables:

$$\tilde{F} = F/F^*, \quad \text{where } F = V, T \text{ or } P,$$

with F*'s being the scaling thermodynamic parameters of the liquid. Assuming the effective occupied volume fraction $V_{o,eff} \geq V_o$, as defined in Eq (4), the hydrodynamic shielding parameter was defined as:

$$h = V_o/V_{o,eff} \tag{6}$$

From Eqs (4)-(6), the temperature dependence of liquid viscosity was predicted to follow the linear dependence:

$$\ln\eta = A + BY \qquad (7)$$

where A and B are parameters, and

$$Y = 1/[h \exp\{0.11515\,(T/T_g)^{3/2}\} - 1] \,.$$

It has been shown that Eq (7) is obeyed by all evaluated liquids including: water, paraffins, aromatics, alcohols, aldehydes, liquified noble gasses, liquid metals, inorganic glasses, polymer melts, etc. (7-9). The adequacy of Eq (7) to describe the concentration effect of polymer solution viscosity was also demonstrated (9).

The usefulness of the Doolittle equation and in consequence Eq (7) disappears when P-effects are concerned (6). If Eq (4) is directly used, instead of a single straight line dependence: $\ln\eta$ vs Y_D, a series of isothermal curves are obtained. If Eq (7) is applied then: (i) again the data do not superimpose, and (ii) the value of $h > 1$ is required to linearize the dependence. The need to use $h \leq 1$ for isobaric and $h > 1$ for isothermic conditions negates the physical significance originally assigned to it.

Before proceeding further, it was necessary to test whether the accepted correlation between η and the free volume fraction, f, exists. Historically, the parameter f was defined (14) as:

$$f = V - \Omega \qquad (8)$$

where Ω was determined by the condition:

$$\lim_{V \to \Omega} \eta = \infty \,. \qquad (9)$$

In the original work (14), it was observed that for non-polymeric liquids:

$$V_s < \omega < V_o$$

where V_S is the molar or specitic volume in the crystalline state. A more precise relation was found between Ω and the critical volume, V_K:

$$3\ \omega/V_K = \Omega/b = 0.921 \pm 0.018 \qquad (10)$$

where b is the van der Waals constant. Since the critical conditions represent a reference point, $P_K V_K/T_K$ = const, it was postulated that Ω can be computed from the equation of state. It is this fundamental principle, the correlation between the transport function, η, and the thermodynamic equation of state quantity, f, which needs to be examined.

In the recent paper (12), the relation between the experimental $\eta = \eta(P, T)$ and the theoretical function $f = f(P, T)$, computed from an equation of state, for n-paraffins C_5 to C_{18} was examined. While the results confirmed the correctness of Batschinski's basic hypothesis, at the same time they demonstrated that neither his nor Doolittle's form of the equation is correct. The data for all n-paraffins examined so far could be described by the relation:

$$\ln \eta/\eta^* = A_1 + B_1/(f + \Delta) \qquad (11)$$

where η* is the vertical shift parameter and A_1, B_1 and Δ = 0.070 are constants of the equation.

In the last publication of this series (15), the applicability to polymeric liquids of the treatment developed for n-paraffins was examined. Four liquids: oligomeric silicone oil, poly(dimethyl siloxane), polypropylene and low density polyethylene, or in brief: SiOil, PDMS, PP and LDPE, respectively, were evaluated. In all but the last case, a single sample was examined. The data in full range of T and P did superimpose on a single curve. There was no effort made to develop an empirical equation between η and f for these

samples. However, the general shape of the dependence indicated that Eq (11), (possibly with different values of $\Delta \gtrsim 0$) could be used.

For LDPE, there were two sets of data. While in each set η (P, T) seemed to follow a single $\eta = \eta(f)$ dependence, these differed for the two sets. The difference was particularly large at large f. As f decreased, the two sets (excepting the samples partially crystallized under pressure) seem to collapse into a single curve; $\eta \doteq 10^7$ (Pa.s). This could be taken as an indication that effects of the molecular weight, polydispersity and structure are losing their importance under high pressure.

In the present paper, the details of the computational procedure for SiOil, PDMS, PP and LDPE will be examined. The procedure will be applied to additional sets of $\eta(P, T)$ data available from the literature. A simple procedure to compute the pressure effects on viscosity will be proposed.

EQUATION OF STATE

The Simha-Somcynsky equation of state (16) has been successfully used in describing P-V-T relations for numerous polymeric and non-polymeric liquids, as well as liquid mixtures (13, 17-28). For polymeric liquids, the general equations can be simplified to read:

$$\tilde{P}\tilde{V}/\tilde{T} = [1 - 2^{-1/6}\, y\, \phi^{1/3}]^{-1} + (2y/\tilde{T})\, \phi^2\, [1.011\, \phi^2 - 1.2045] \qquad (12)$$

$$[1 + y^{-1}\ln(1-y)] = (y/6T)\, \phi^2\, [2.409 - 3.033\, \phi^2]$$

$$+ [2^{-1/6}\, y\, \phi^{1/3} - \tfrac{1}{2}][1 - 2^{-1/6}\, y\, \phi^{1/3}]^{-1} \qquad (13)$$

where: $\phi = 1/(yV)$ and $y = 1 - f$.

To compute $f(\tilde{P}, \tilde{T})$ from the coupled Eqs (12) and (13), first the reducing parameters, F*'s, have to be determined. Once these are

known, then for each T the Equations (12) and (13) can be solved. The computation starts by setting $\tilde{P} = 0$, to determine the initial values of $\tilde{V}$, y and $Y_s \equiv 1/(1-y)$. Next, the coupled equations are solved for $\tilde{P}$, y and Y_s at constant, selected intervals: $\delta = \ln(\tilde{V}_{i+1}/\tilde{V}_i)$. To determine Y_s at the appropriate, experimental value of P a polynominal interpolation method is used. As a result, to each experimental data point $n(P_i, T_i)$ a corresponding packing parameter $Y_s(\tilde{P}_i, \tilde{T}_i)$ (per definition $\tilde{P}_i = P_i/P^*$ and $\tilde{T}_i = T_i/T^*$) is assigned.

The method of determination of the reducing parameters was detailed previously (12). Briefly, for polymer melts the method involves two steps:

(1) Determination of V* and T* from the isobaric V-T data.

(2) Computation of P*.

In the first step, one makes use of the approximate Eq (5) with $S_o = -0.10335$ and $S_1 = 23.8345$ (6). The values of $\tilde{V}$ computed from Eq (5) are within 0.16% from those computed directly from the coupled Eqs (12)-(13) at $\tilde{P} = 0$ in the range: $1.65 \leq \tilde{T}.10^2 \leq 7.03$. Comparing the experimental values of the parameters in the empirical dependence:

$$\ln V = Z_o + Z_1 T^{3/2} , \qquad (14)$$

with S_o and S_1 , one finds that:

$$V^* = \exp (Z_o - S_o) , \qquad (15a)$$

and

$$T^* = (S_1/Z_1)^{2/3} . \qquad (15b)$$

It should be stressed that the above quoted values of S_o and S_1 were determined by solving Eqs (12)-(13) at P = 0. Obviously, V* and T* should not depend on the assumed isobaric conditions, as long as these are identical for V-T experiments and for the computation

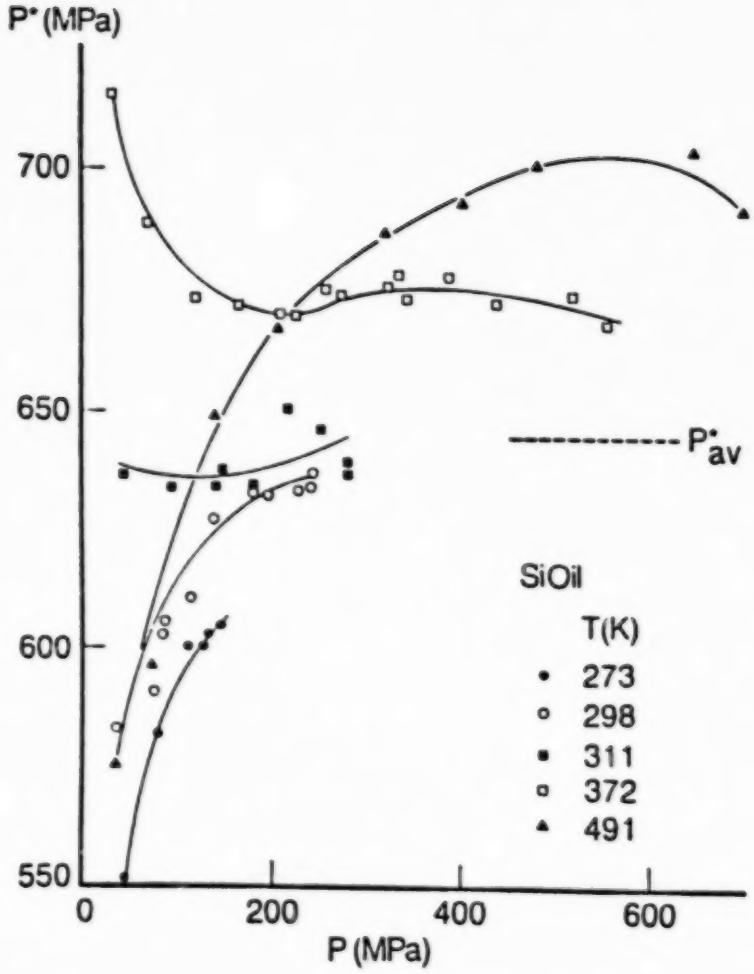

Fig. 1 Computed P* vs P at the T indicated; the average value, P_{av}^*, is also marked. SiOil (29).

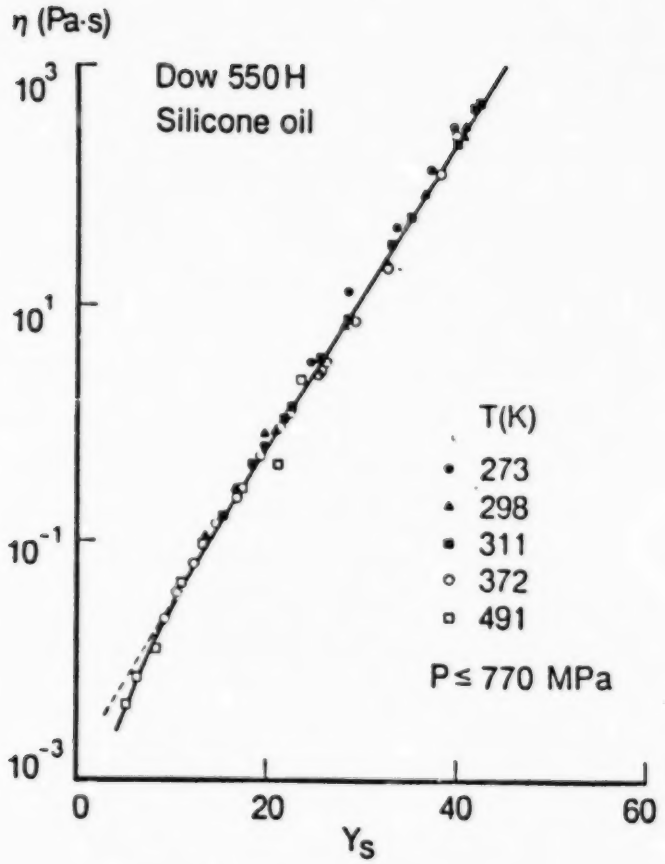

Fig. 2 Viscosity of SiOil vs Y_s at T = 273 to 491 K and P ≤ 770 MPa (29).

of S_o and S_1.

In the second step, $\tilde{V}$ and $\tilde{P}$ are computed from Eqs (12)-(13) at the experimentally defined $\tilde{T}_i = T_i/T^*$. Since V* is known, then experimental values of $\tilde{V}_i = V_i/V^*$ are known and the corresponding $\tilde{P}_i$ can be determined. Since P_i (corresponding to T_i and V_i) is also known, then P_i^* can be computed from each P-V-T point. Usually, these P_i^*'s are averaged to obtain the final P* value.

EVALUATION

1. SiOil. The viscosity, η, and density, ρ, of in a range of P = 0 to 770 MPa and T = 273 to 419 K (29). The plot of the ambiant pressure density vs temperature permitted calculation of:
$Z_o = -0.192415$, $Z_1 = 2.416039 \cdot 10^5$ with the correlation coefficient squared $r^2 = 0.998646$. From these values: T* = 9967 K and $V^* = 9.162 \cdot 10^{-4}$ (m^3/kg) were found. Next, from the actual ρ-T-P data, 51 values of P* were computed. These values are presented in Fig. 1 as P* vs P at T = const. The arithmetic average: $P_{av}^* = 644.4 \pm 38.3$ MPa was taken for the subsequent computation of $Y_s(\tilde{P}, \tilde{T})$.

The empirical values of η as reported in (29) are plotted in Fig. 2 vs the computed crowding (or packing) parameter $Y_s = 1/f$. It is worth noting that for SiOil, using Eq (4), where Y_s replaced Y_D, a good description of η-P-T behaviour is obtained. Here, in the range of $6.5 < Y_s < 42$, or η spanning five decades, log η is a linear function of Y_s.

Such a good superposition of data is unexpected in view of the uncertainty in determining P* (see Fig. 1). It seems that the main sources of P*-variability are the experimental errors and/or the approximations used during the computation procedure of F*'s as

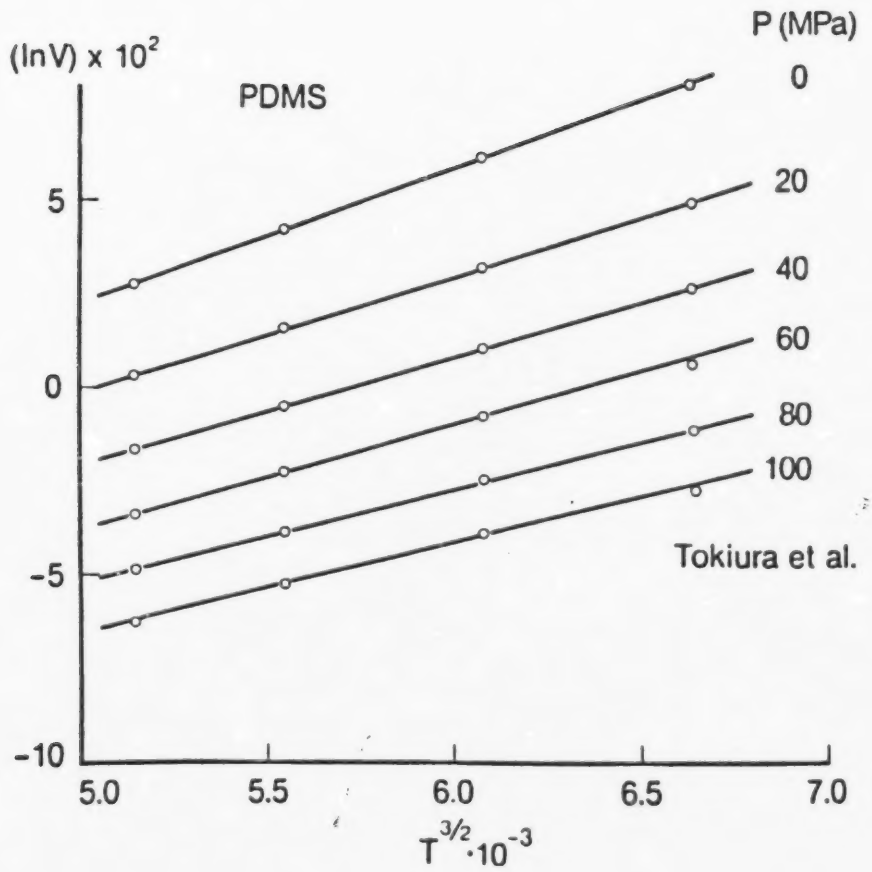

Fig. 3 Isobaric plot of the experimental V-T data for PDMS (30) according to Eq (14); T = 298-353 K and P ⩽ 100 MPa.

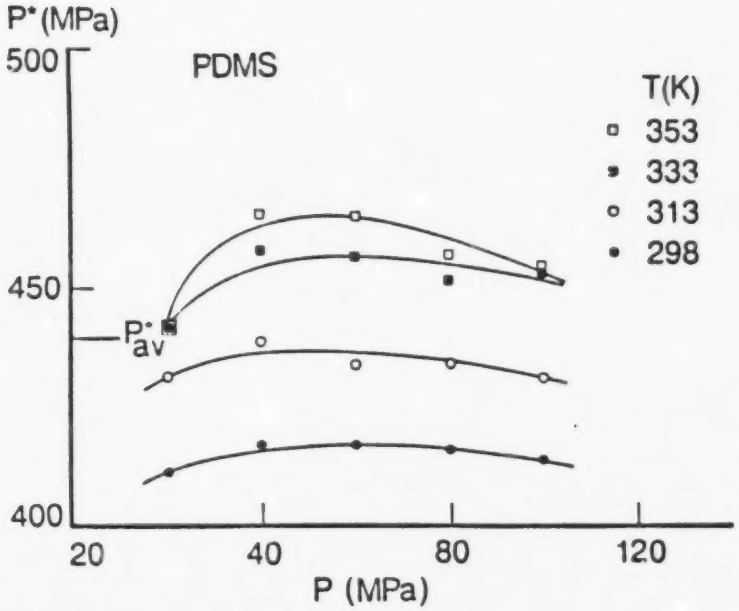

Fig. 4 Computed P* vs P at the T indicated; average value, P_{av}^*, is marked. PDMS (30).

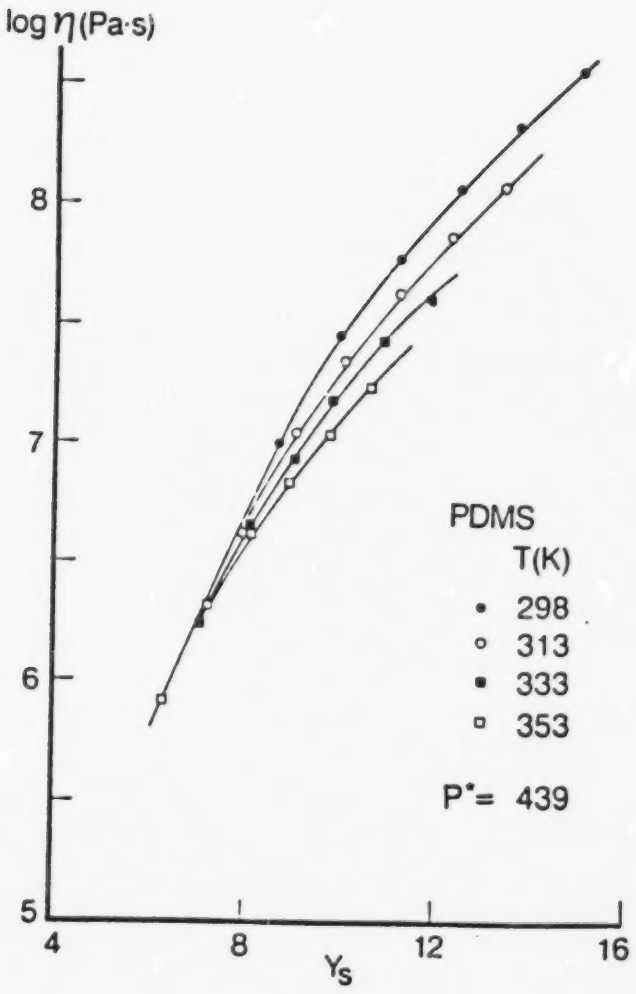

Fig. 5 $\eta - Y_s$ relation for PDMS at the T indicated and $P \leq 100$ MPa (30). Y_s computed assuming $P_r^* = P^*$.

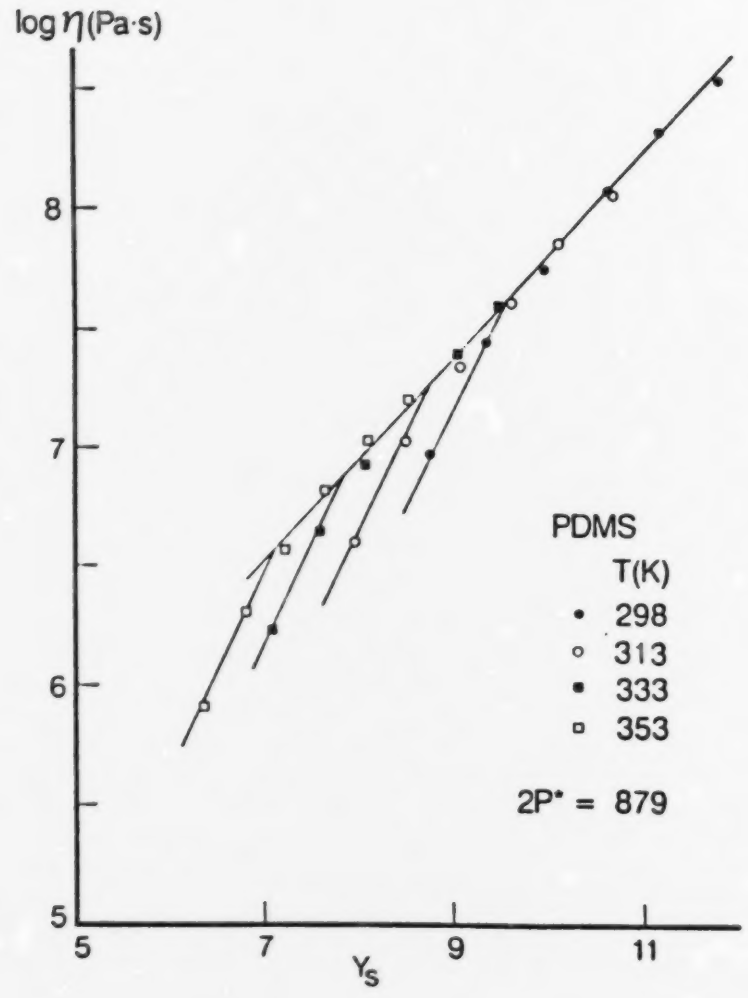

Fig. 6 The same data as in Fig. 5; here $P_r^* = 2P^*$ was assumed.

introduced by use of Eqs. (5) and (15). Both the P-V-T relation computed from Eqs (12-13) and the superposition of $\eta(P,T) = f(Y_s)$ demonstrate the soundness of the basic thermodynamic theory.

II. PDMS. The viscosities and specific volumes for commercial poly(dimethyl siloxane), PDMS, were reported by Tokiura et al. (30). The sample with the viscosity average molecular weight, M_v = 234,000 was measured at T = 298 to 353 (K) and P = 0 to 100 MPa. The plot lnV vs $T^{3/2}$ is shown in Fig. 3. The least-squares fit to P=0 data gives: $Z_o = -0.15074$ and $Z_1 = 3.47971 \cdot 10^5$ with $r^2 = 0.99963$, from which T* = 7770.4 K and V* = 9.537×10^{-4} (m^3/kg) were calculated. The plot of P* vs P at T = const. is shown in Fig. 4. The average value P* = 439 ± 18 was computed. The plot of lnη vs Y_s is shown in Fig. 5. It is apparent that instead of one master curve there are clearly four isothermal dependencies i.e. apparently the unique correlation between η and f does not exist for this system. The maximum spread of η at Y_s = constant is about 30%. While this is not a large error for melt viscosity data (see DISCUSSION), the systematic variability would be difficult to explain by inaccuracies in the measurements. It seems that the reason for lack of superposition comes not from η but Y_s.

It is worth noting that to calculate $Y_s(\hat{T}, \hat{P}) = Y_s(\hat{T}, \hat{V})$ the knowledge of the average P* is not necessary; once $\hat{T}$ and $\hat{V}$ are known, Y_s can be found. Such a treatment is equivalent to assuming an individual value of P_i* for each data point. For PDMS, this alternative method did not significantly improve the superposition. One has to conclude that for polymer melts the thermodynamic f is not necessarily identical to the rheological one. The simplest way to incorporate this concept is by allowing the rheological scaling pressure $P_r^* \neq P^*$. As can be seen in Fig. 6 $P_r^* = 2P^*$ was required to generate a good superposition of the high viscosity data. However, in this case no superposition was obtained for low-η values.

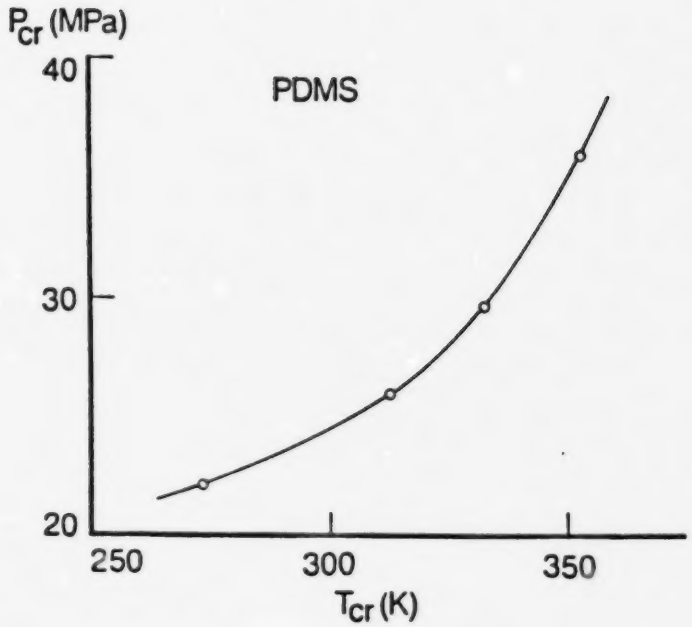

Fig. 7 The critical parameters P_{cr} vs T_{cr} for PDMS, as determined by intersection of the straight line dependencies ln η vs Y_s in Figs. 5 and 6.

It seems that PDMS exists in two different liquid forms: a low viscosity one for which the thermodynamic P* provides a good master curve, and a high viscosity one for which $P_r^* = 2P^*$ is required to obtain superposition. The transition between them is defined by: T_{cr}, P_{cr}, ploted in Fig. 7.

The well known Tait relation (31) can be cast into a reduced parameter form (32):

$$1 - \tilde{V}(\tilde{P},\tilde{T})/\tilde{V}(0,\tilde{T}) = C \ln [1+\tilde{P}/\tilde{B}(\tilde{T})] \qquad (14)$$

where the "universal constant", C = 0.0894 and B is the "Tait parameter" which depends only on T:

$$\tilde{B}(\tilde{T}) = B(T)/P^* \quad . \qquad (15)$$

B can be directly computed from the coupled Eqs (12)-(13) using Eq (14) as the definition. Calculated in this manner $\tilde{B}$ decreases with $\tilde{P}$ by about 4% (Table 1).

TABLE 1 Computed values of B for PDMA at P=0-100 MPa

No	T(K)	$\tilde{B}$ (range)	$\tilde{B}$ (average)	B (ref. 30)	P* (MPa)
1	298	0.149-0.145	0.147	78.97	537
2	313	0.137-0.132	0.135	73.82	548
3	333	0.123-0.117	0.120	67.47	562
4	353	0.110-0.103	0.107	61.67	577
				P* (average)	556

Using the average values of $\tilde{B}$, P* can be calculated from Eq (15);

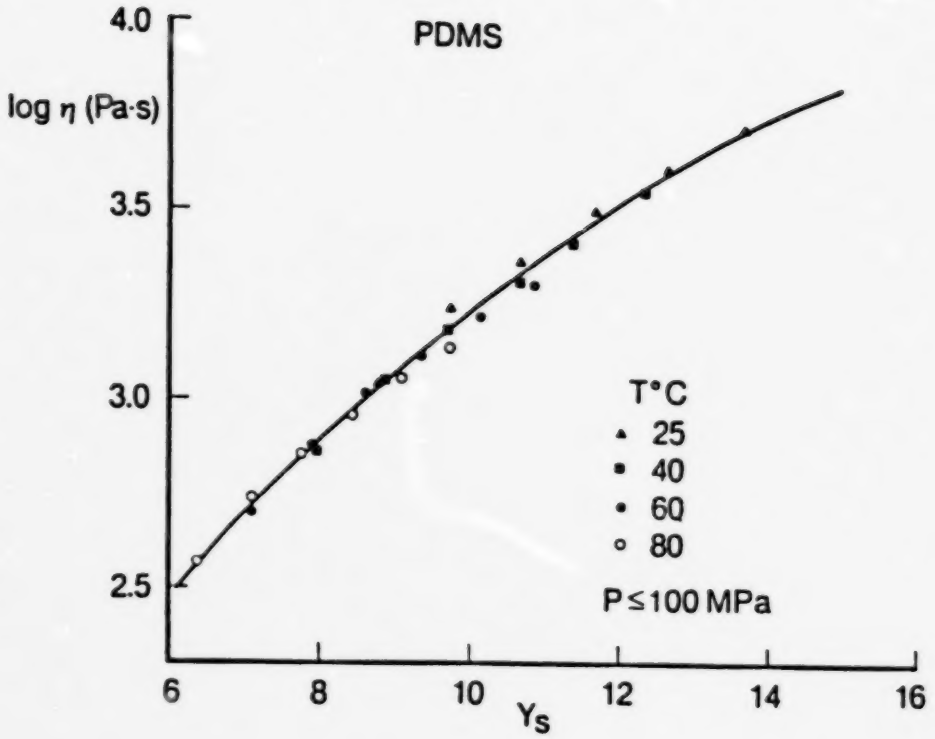

Fig. 8 ln η vs Y_s for PDMS (30); P* used in calculation of Y_s was obtained from the Tait parameter B.

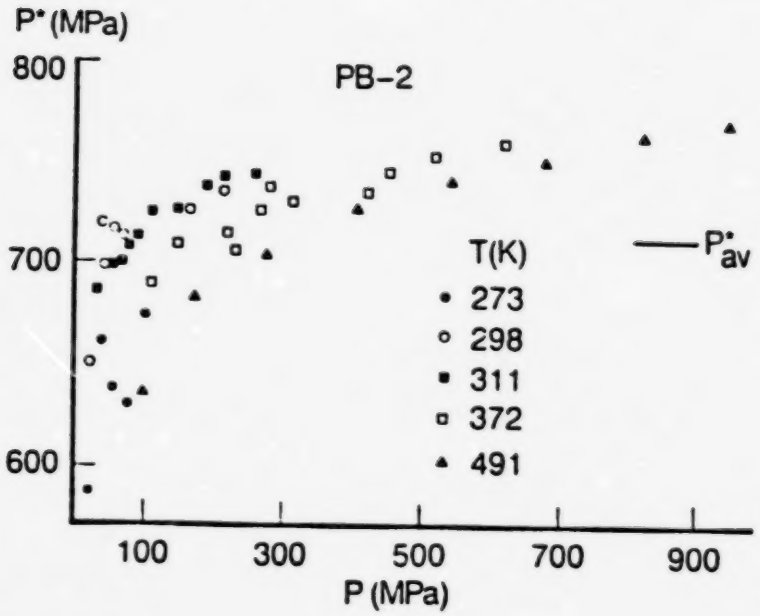

Fig. 9 Computed P* vs P at the T indicated for PB-2; average value, P_{av}*, is also marked (29).

these values are also listed in Table 1. It can be seen that there is a large difference between P*=439±18 calculated directly from P-V-T data and P*=556±17 calculated from the Tait parameter. When the latter value is used to compute Y_s the resulting Fig. 8 shows a better clustering of data-points around a common dependence, but close scrutiny reveals a systematic tendency noted in Figs. 5 and 6. Discussion on the subject will continue after PB-Oils behaviour is analyzed (next chapter).

III. PB-Oils. Three poly(butylene) oils were measured (29). The samples, labeled here: PB-1, PB-2 and PB-3 (in order of increasing molecular weight, MW) were low MW lubricating oils. The reported MW = 645±10 of PB-3 suggests the formula: $C_{46}H_{94}$. Both η and ρ were measured at T = 273 to 491 (K) and P=0 to 1000 (MPa).

First, the P-V-T dependencies were examined. As before, V* and T* were computed (see Table 2) then P*'s calculated from each individual P-V-T data point. An example of P* vs P at T = const. is shown in Fig. 9. The average values are listed in Table 2.

TABLE 2 Scaling parameters for PB-Oils

Sample	$V^*.10^3(m^3/kg)$	T*(K)	P*(MPa)
PB-1	1.145	9019	767
PB-2	1.136	9049	713±40
PB-3	1.132	9306	767

In spite of variability of P* the adequacy of Eqs (12)-(13) to describe the P-V-T dependence is excellent. The theoretical curves

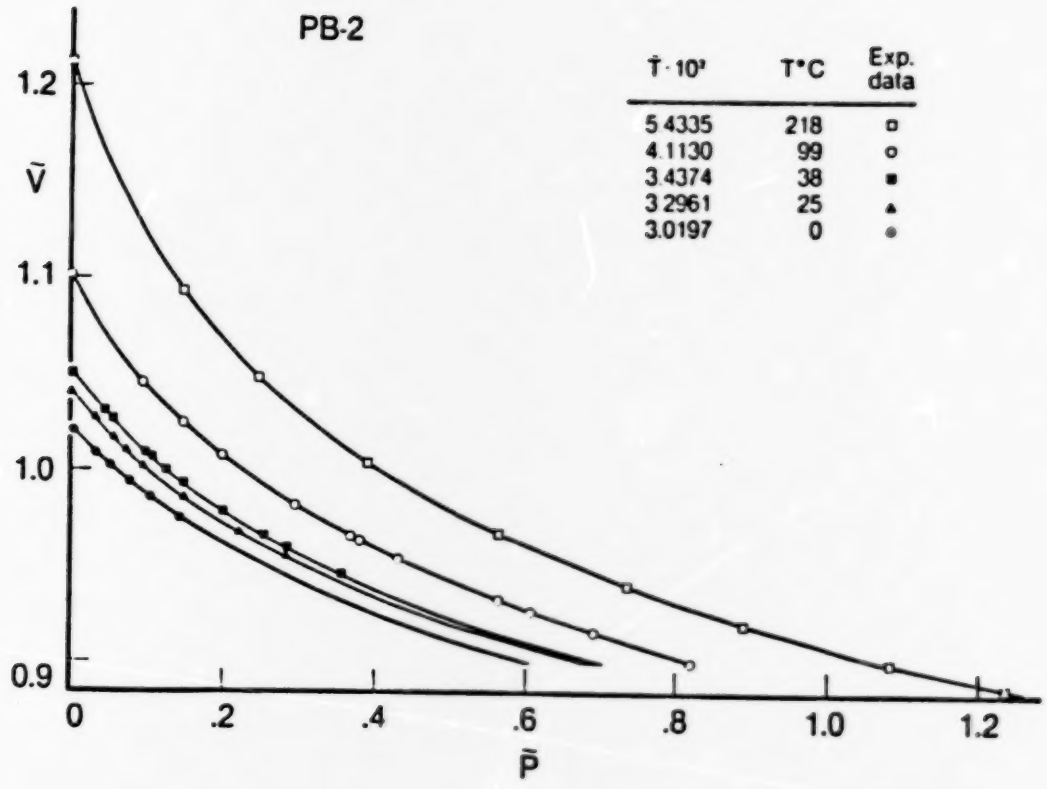

Fig. 10 Experimental (points) and computed from Eqs (12, 13) $\tilde{V}$-$\tilde{P}$ at $\tilde{T}$ = const for PB-2 (29); for clarity most of the points at lower $\tilde{V}$ were omited.

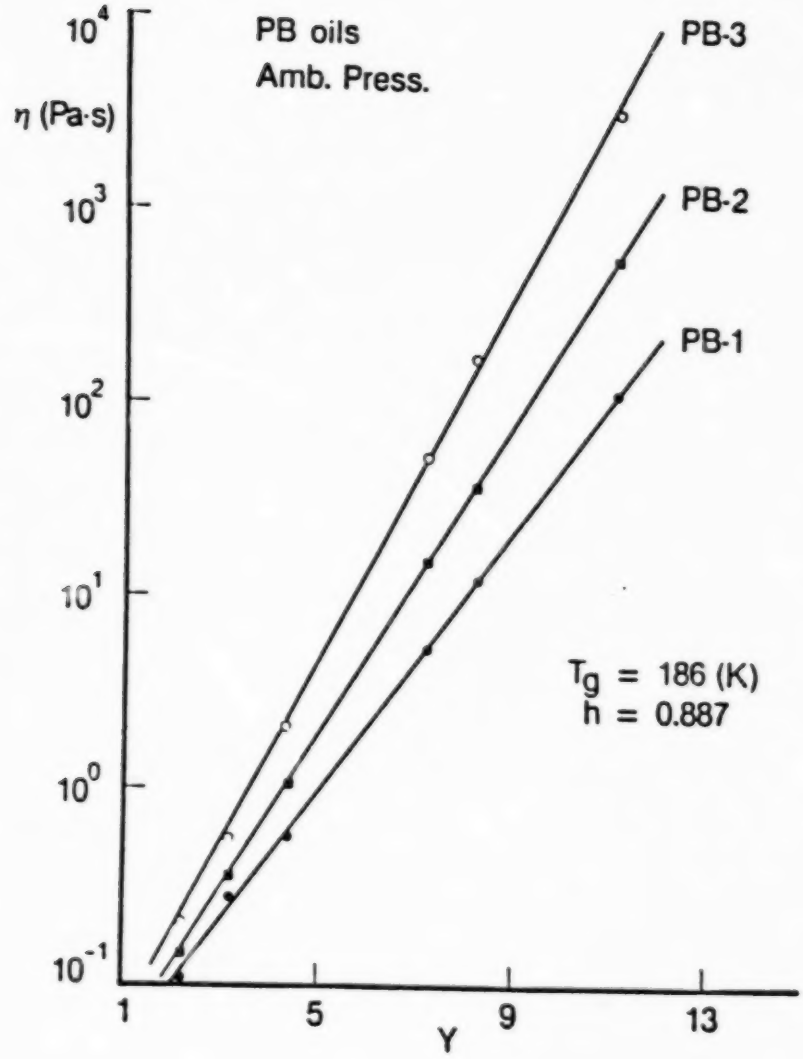

Fig. 11 Linearization of ambiant pressure η-T dependence for PB (29) by means of Eq (7).

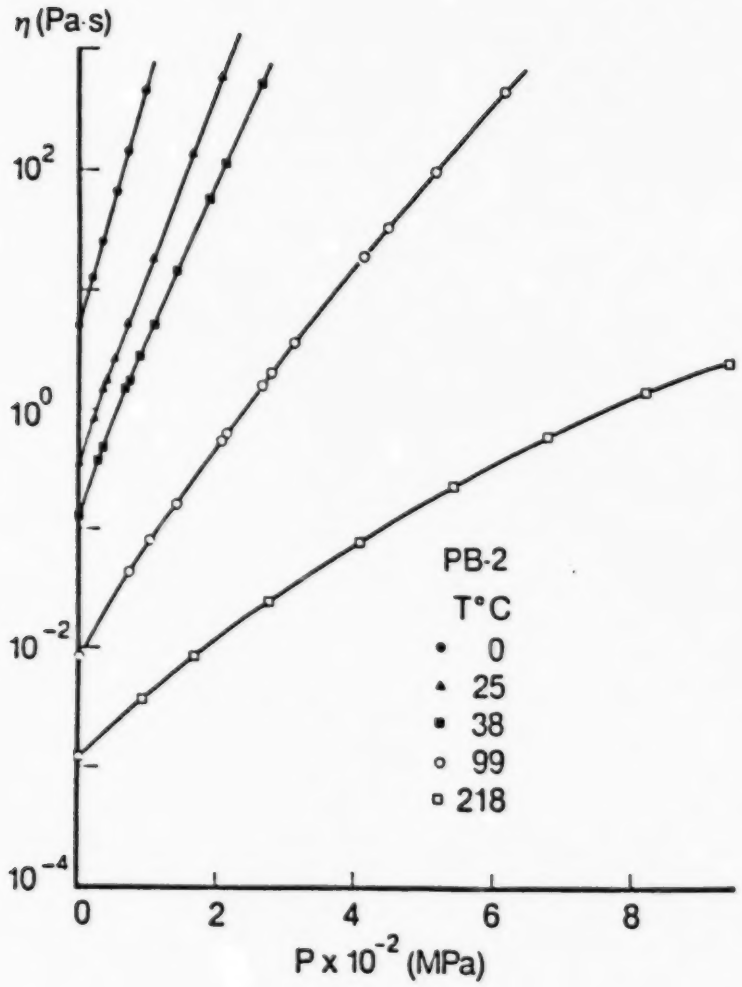

Fig. 12 Experimental isothermal η-P dependencies for PB-2 at the T indicated (29).

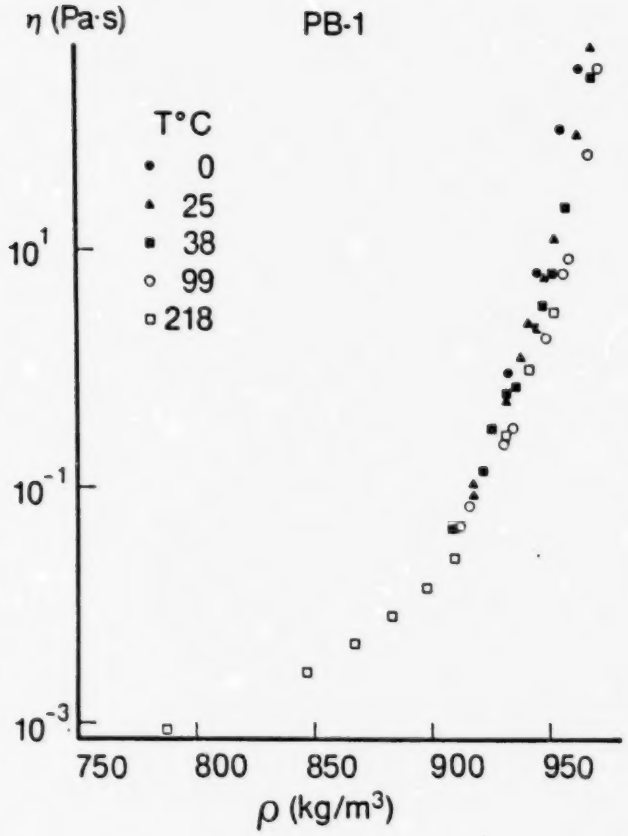

Fig. 13 Experimental plot of viscosity vs density, $\rho = \rho(P, T)$, for PB-1 (29); T = 273-491 K, $P \leq 1$ GPa.

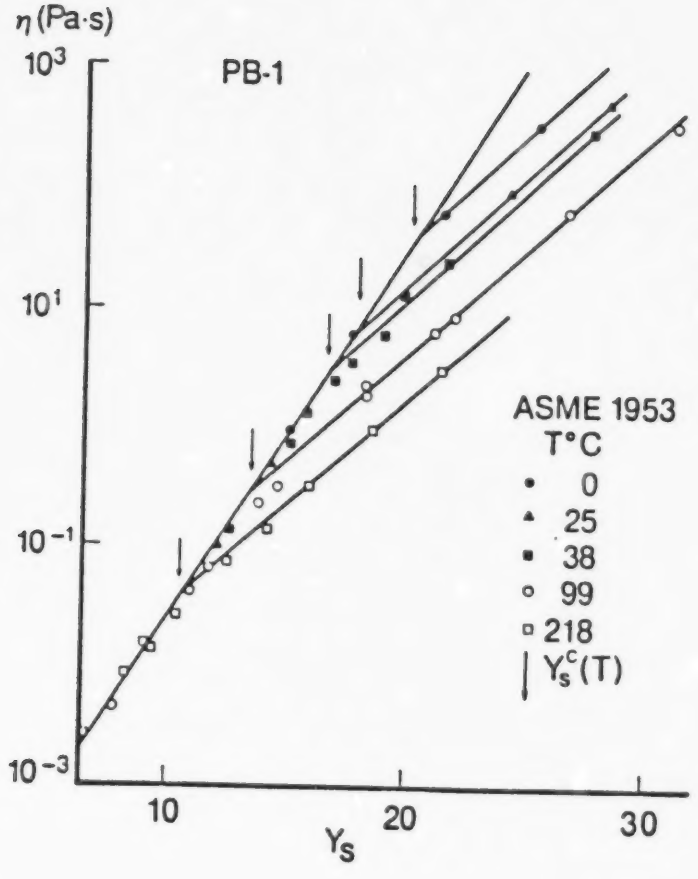

Fig. 14 η-Y_s dependence for PB-1 (29); $P_r^* = P^*$ was assumed.

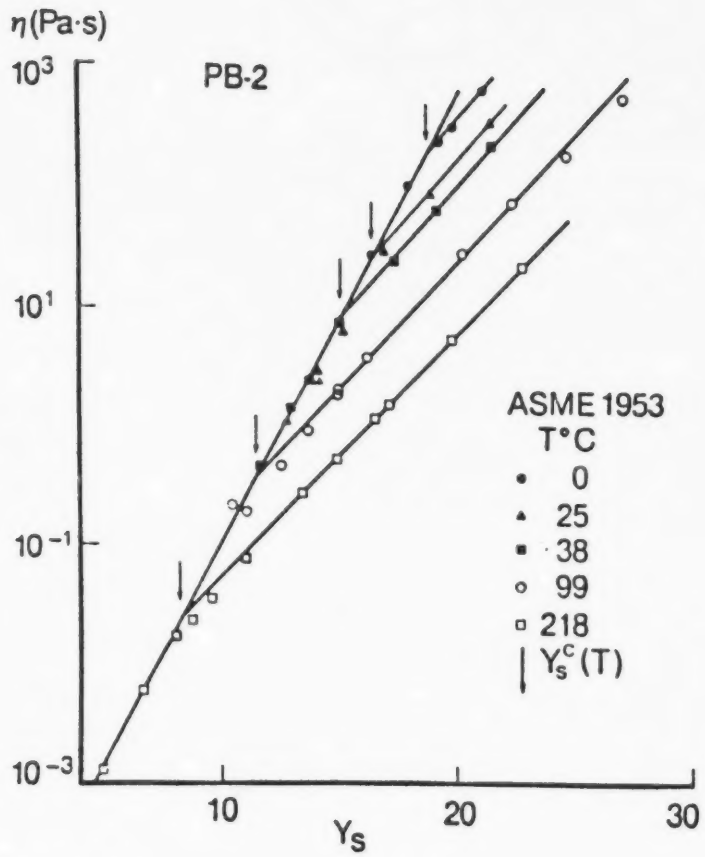

Fig. 15 η-Y_s dependence for PB-2 (29); $P_r^* = P^*$ was assumed.

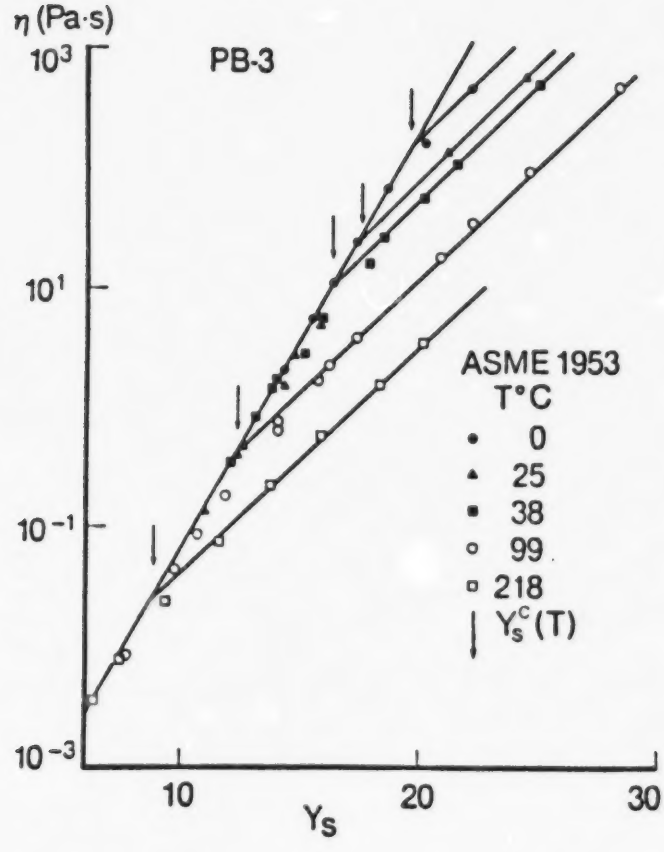

Fig. 16 η-Y_s dependence for PB-3 (29); $P_r^* = P^*$ was assumed.

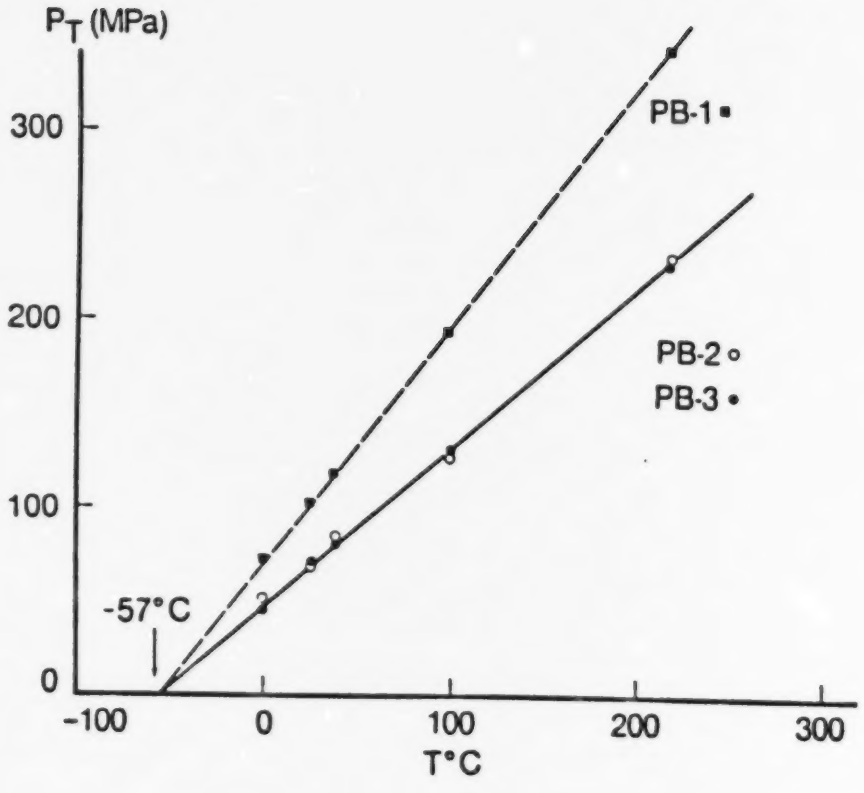

Fig. 17 The critical parameters $P_T = P_{cr}$ vs $T_T = T_{cr}$ for PB as determined by intersects of the straight lines ln η vs γ_s in Figs. 14 to 16.

are well within the range of experimental accuracy for all three samples in the full range of variables. An example of $\tilde{V}$ vs $\tilde{P}$ at $\tilde{T}$ = const. is shown in Fig. 10.

Next the ambiant pressure viscosity was analyzed using Eq (7). The results are presented in Fig. 11; good linearization with a reasonable value of the shielding parameter, h=0.887, was obtained.

The pressure dependence of η is illustrated in Fig. 12 as log η vs P for PB-2 and Fig. 13 as log η vs ρ for PB-1. Finally, in Figs 14-16 the dependence log η vs Y_s is shown. In Fig 12, the η smoothly increases with P; this indicates absence of random experimental errors. The consistency of results in Fig. 13 is worse, suggesting that ρ-measurements may not be as precise. However, the plots in Figs. 14-16 show a lack of superposition. This behaviour, similar to that observed for PDMS, cannot be explained either by experimental error or the P* variability. The spread of η's for PB-oils at Y_s = const. is much larger - a factor of about 22 is involved.

The arrows in Figs. 14-16 indicate the "transition" in flow behaviour. The values of $P_{cr} = P_T$ at which the break occurs at each T are presented in Fig. 17. The dependence is linear, extrapolating to a common point: T_T = 216(K) at P=0. Should the behaviour observed in Figs. 14-16 be due to a transition, then this would be observed at ambiant pressure at T_T. The glass transition temperature, T_g = 189 (K) can be calculated from T_g (MW → ∞) = 249 (K) (33) and the empirical dependence (34):

$$T_g = T_g(\infty) - 3.87.10^4/MW \ . \qquad (16)$$

The ratio T_T/T_g = 1.14 is within the limit of the ratio $R_{LL} = T_{LL}/T_g$ = 1.13 for polypropylene to 1.19 for polyhexene (35). Furthermore, from the relation (36):

$$D = dT_{LL}/dP(MPa) = 280/T_g - 0.2 \qquad (17)$$

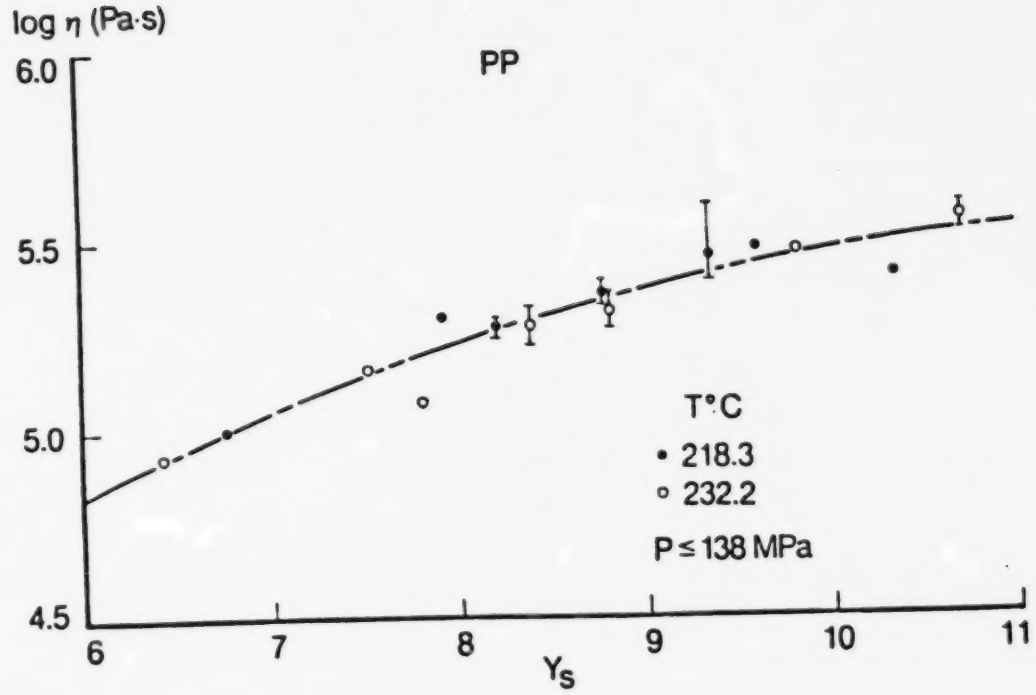

Fig. 18 $\eta - Y_s$ dependence for PP at T = 487 and 506 K and P ≤ 138 MPa (37); $P_t^* = P^*$ was assumed.

D = 1.28, to be compared with the experimental value (Fig. 17) of 1.18 ± 0.01. This is a reasonable agreement considering the experimental uncertainty and the approximate nature of Eqs (16), (17). In short, T_T can be identified with the T_{LL} transition temperature.

It is worth recalling that the discontinuity in η - T and η - c have been previously reported for a number of liquids (7-10). The discontinuity in η - P is not an oddity but a natural consequence of the existence of different liquid structures.

The break in lnη vs Y_s for PDMS was also noted. However, judging by the data in Fig. 7 the transition under ambiant pressure should be observed at T < 250 K. If indeed the observed transition is of the liquid-liquid type, then this should not be a surprise; T_g = 146 K for PDMS and if R_{LL} = 1.1 to 1.2 then $T_{LL} \doteq$ 160 to 175 K is to be expected.

IV. PP. Hercules Pro-fax 6523 propylene, PP, was investigated at T = 487 to 506 (K) and at P = 0 to 138 (MPa) (37). Because of the limited range of variables, the F*'s were taken from Zoller (38): p* = 542 (MPa), T* = 11155 (K) and V* = $1.195 \cdot 10^{-3}$ (m^3/kg). The η - Y_s dependence is shown in Fig. 18. Since the authors provided η-values for repetitive runs, the bars indicate the experimental spread of data. There is no systematic variation between the two isothermal sets. It is apparent that within the experimental error the results follow a "master curve".

For PP (35): T_g = 264.5, T_{LL} = 298 at P=0 and its value at P = 138 (MPa) can be calculated from Eq (17) as T_{LL} = 416 (K). This indicates that the η-measurements were carried out at T > T_{LL}, within a single liquid structure. Because of limited range of T and a large scatter of data the calculations were not repeated for $P_r^* = 2\ P^*$.

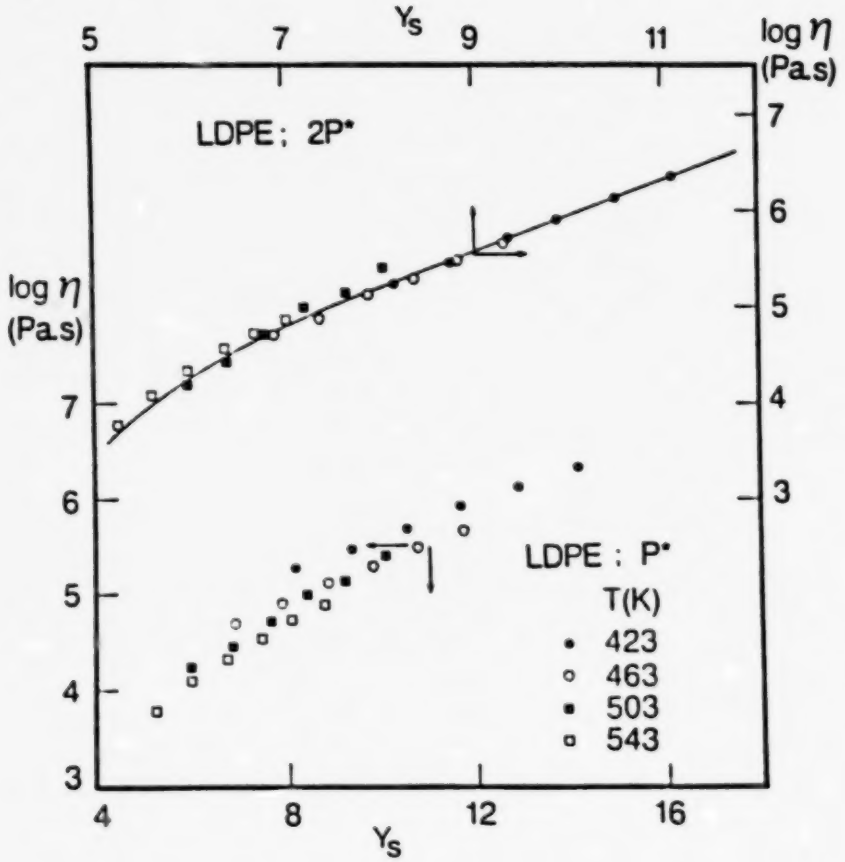

Fig. 19 $\eta - Y_s$ dependence for LDPE (39) at T = 423 to 543 K and $P \leq 175$ MPa; for the lower set of points $P_r^* = P^*$ and for the upper $P_r^* = 2P^*$ were assumed.

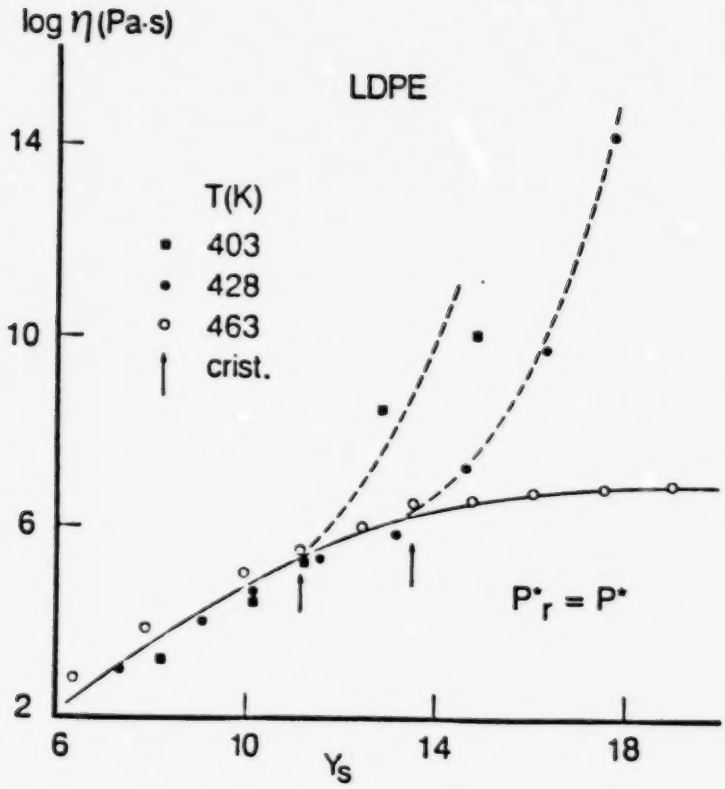

Fig. 20 $\eta - Y_s$ dependence for LDPE (40) at T = 403 to 463 K and P < 500 MPa; $P_r^* = P^*$ was assumed. The arrows indicate onset of crystallization at the two lower temperatures.

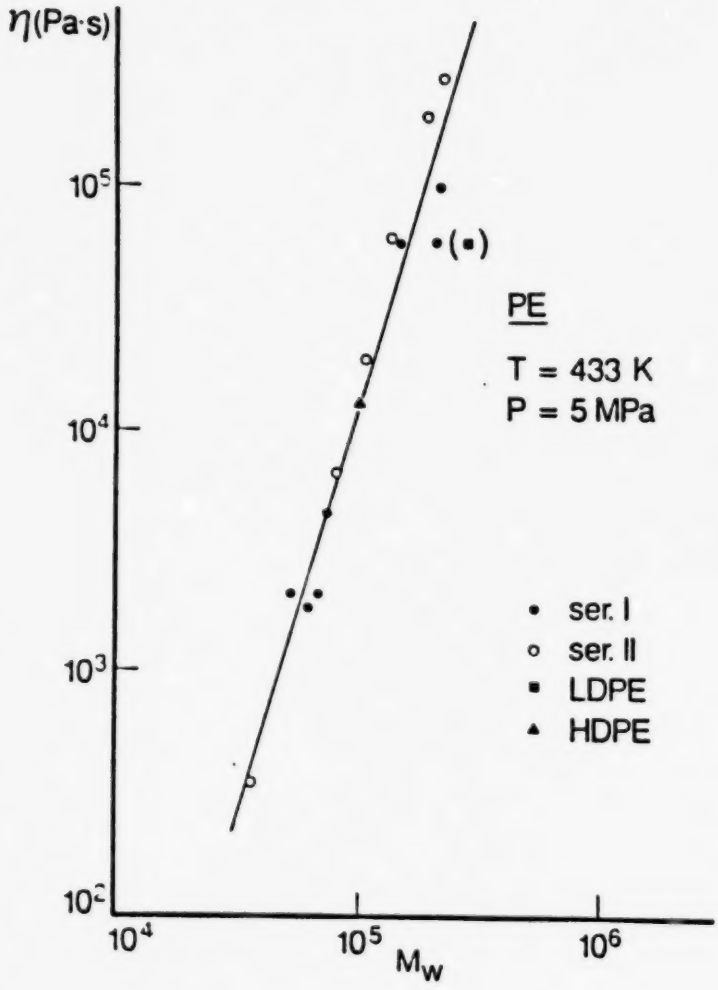

Fig. 21 $\eta - M_w$ correlation for various polyethylenes (see text) at T = 433 K and P = 5 MPa (41, 42). The line represents Eq (18).

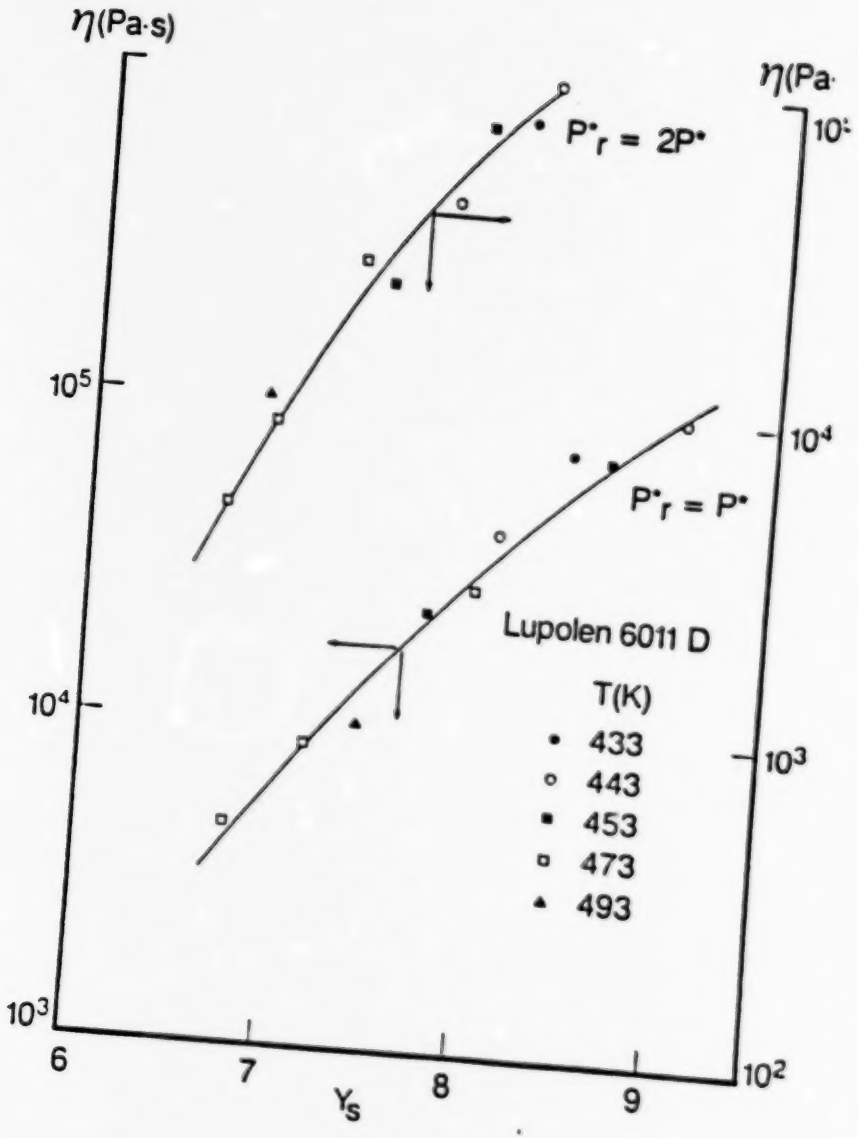

Fig. 22 $\eta - Y_s$ for Lupolen 6011D (41, 42) at T = 433 to 493 and P < 50 MPa; both values $P_r^* = P^*$ (lower set) and $P_r^* = 2P^*$ (upper set) were assumed. The lines represent second order polynominals.

V. LDPE. The data on low density polyethylene, LDPE, were reported by Cogswell et al. (39), Karl (40) and Christman et al. (41, 42). These will be discussed separately.

V.1. Cogswell and McGowan (39) reported ηat T = 423 to 543 (K) and P = 0 to 175 MPa. To compute Y_s the F*'s were taken from (32): P* = 729 (MPa), V* = 1.167 x 10^{-3} (m^3/kg) and T* = 10620 (K). The results are presented in the lower part of Fig. 19; in the upper part the same data are plotted vs Y_s computed, assuming P_r^* = 2 P*. The latter plot indicates better superposition.

V.2. Karl (40) measured one sample at T = 403, 428 and 463 (K) and P = 0 to 500 MPa. In the capillary flow shear crystallization was observed at the two lower temperatures. Since the density, ρ, vs P data were not measured the F*'s were taken from (32). The results of computations are presented in Fig. 20.

V.3. Christman et al. (41, 42), using four different rheometers measured two series of PE's: I with the $M_n \doteq 12{,}000$ and variable M_w/M_n, and II with $M_w/M_n \doteq 6$ and variable M_w (Table 3). The η-data were determined at T = 413 to 493 (K) and P = 5 to 50 (MPa). Excepting the two commercial resins, Lupolen and Hostalen, the other samples were special products. Lupolen is LDPE, Hostalen with ρ = 947 kg/m^3 high density polyethylene, HDPE, the others of unknown type. The plot of η vs M_w (Fig. 21) permits the expression:

$$\eta = 2.12 \cdot 10^{-13} M_w^{3.35} \quad ; \quad r^2 = 0.950 \qquad (18)$$

for all but the Lupolen, samples. On this basis, it seems reasonable to assume that most of the tested PE's were of the HDPE-type. These will be discussed latter.

In Fig. 22, η vs Y_s is shown for sample I/9. Here, to calculate Y_s, the F*'s were taken from (32). Both P_r^* = P* and P_r^* = 2 P* were used. The fit in both cases is good, although the

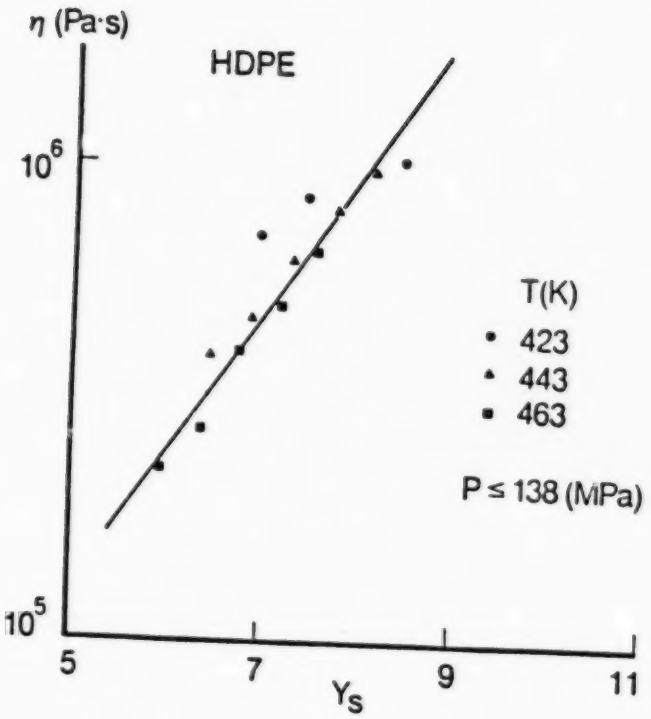

Fig. 23 $\eta - Y_s$ for HDPE (39) at T = 423 to 463 K and P $\lesssim$ 138 MPa; $P_r^* = 2P^*$ was assumed.

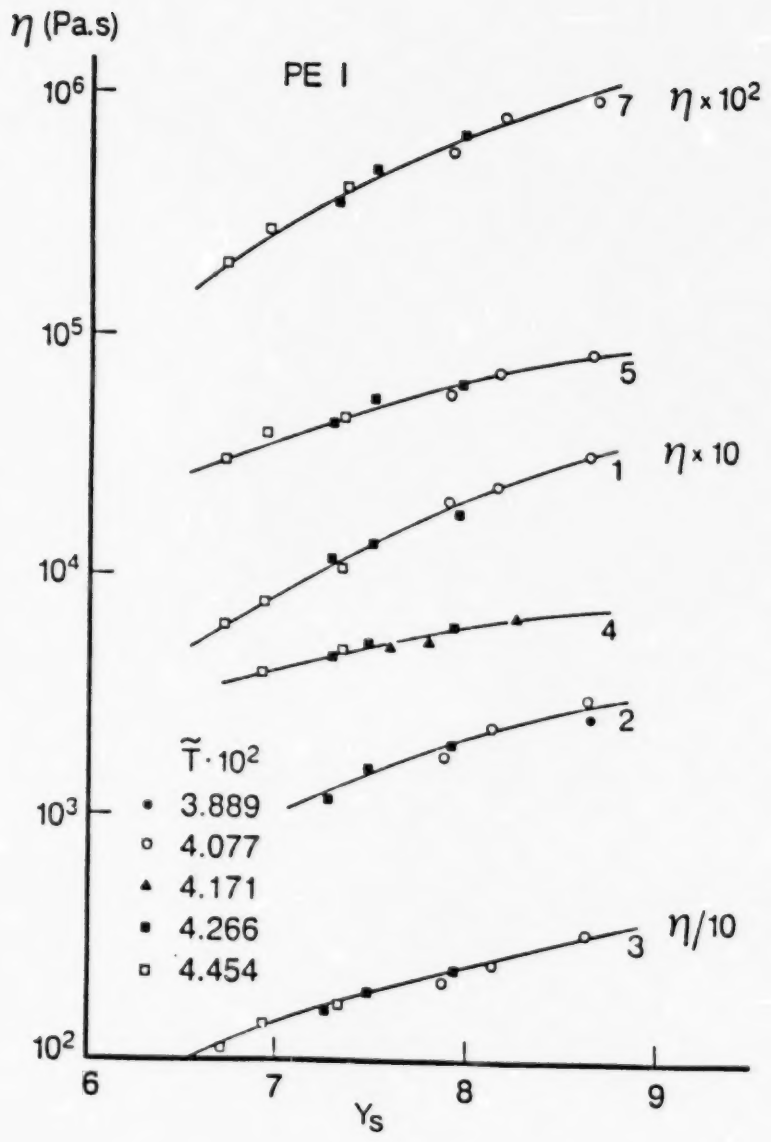

Fig. 24 $\eta - Y_s$ dependence for the first series of polyethylenes (41, 42) in which M_n was relatively constant and polydispersity changed (Table 3); T = 423 to 493 K and P $\leq$ 50 MPa. $P_r^* = 2\,P^*$ was assumed.

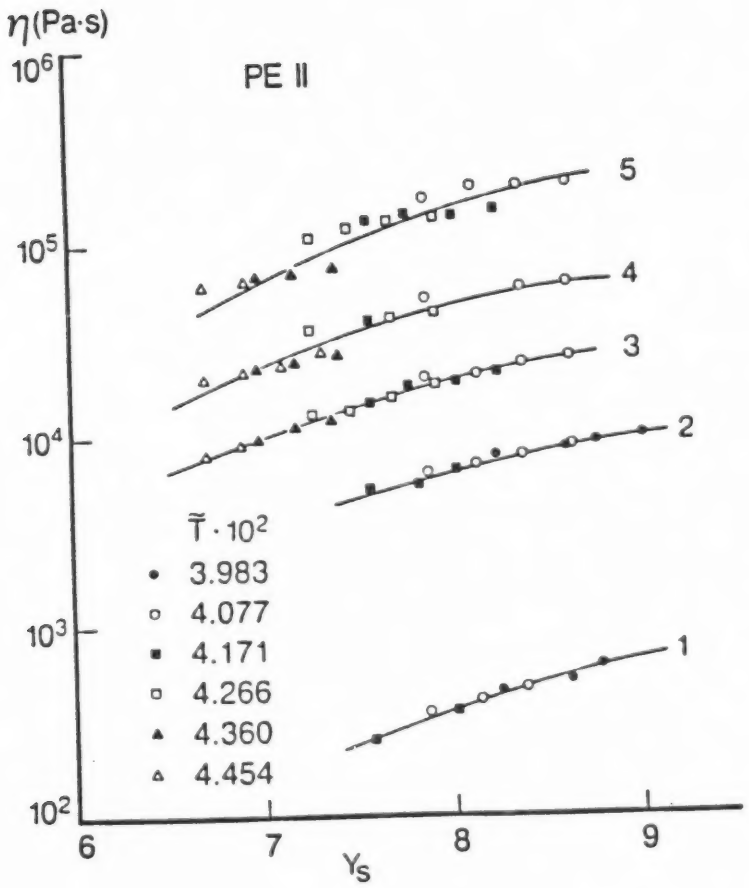

Fig. 25 $\eta - Y_s$ dependence for the second series of polyethylenes (41, 42) in which polydispersity was nearly constant (M_w/M_n = 5 to 6) and M_w varied; T = 413 to 493, P ≤ 50 MPa and $P_r^* = 2P^*$.

second order curve fit in the first case is better (r^2 = 0.996) than in the second (r^2 = 0.987).

VI. HDPE. Here, two sources of η-P-T data are available; those of Cogswell and McGowan (39) and of Christman and Knappe (41, 42). For both sets the F*'s were taken from (32). In both cases the two assumptions: $P_r^* = P^*$ and $P_r^* = 2\,P^*$ were examined. The results presented in Figs. 24-25 are those obtained for the second case.

As can be seen in Fig. 23, the low temperature data (39) show significant scatter; the other viscosities seem to follow Y_s quite well.

Table 3. Characteristics of PE samples (41, 42).

Series	N°	$M_n\ 10^{-3}$	$M_w\ 10^{-3}$	M_w/M_n	Type
I	1	14	52	3.7	
	2	12	62	5.2	
	3	12	69	5.8	
	4	9.8	73	7.4	
	5	22	210	9.6	
	6	12	100	∿11.0	Hostalen GD6250, HDPE
	7	12	150	12.5	
	8	15	220	14.6	
	9	12	280	∿21.0	Lupolen 6011D, LDPE
II	1		36.6	5 to 6	
	2		81.5	"	
	3		103	"	
	4		138	"	
	5		197	"	
	6		223	"	

In Figs. 24 and 25, the data for the two series of PE's (41, 42) are presented. In both cases, a good fit to a single master curve is found. For PE I, the data for constant M_n and variable M_w/M_n are presented in Fig. 24. As the polydispersity increases

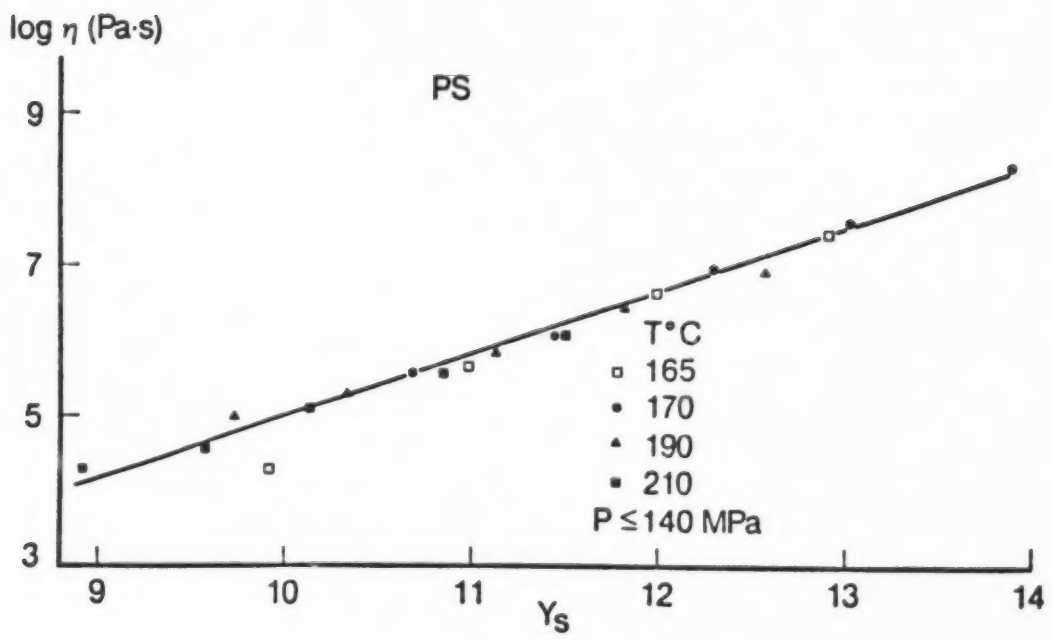

Fig. 26 $\eta - Y_s$ dependence for PS (39) at T = 443 to 483 K and P $\leqslant$ 140 MPa; $P_r^* = 2P^*$ was assumed.

the slope

$$D \equiv d \ln \eta / d Y_s \qquad (19)$$

decreases. An exception is sample I/7 with a much steeper increase than expected on the basis of its M_w/M_n = 12.5. For PE II, where M_w/M_n remains constant and M_w changes, the data in Fig. 25 for the three lowest M_w samples follow the "master curve", but those of $M_w \geq 138{,}000$ show poor overlapping. The experimental values, as reported by the authors, change little with P; e.g. at 453 K and P varying from 5 to 20, 35 and 50 MPa $\eta x 10^5$ (Pa.s) varies: from 1.2 to 1.2, 1.3 and 1.3 respectively. i.e. is nearly constant within the range of experimental errors. Considering the other data on η-P dependence of HDPE presented in Figs. 23 and 24, it seems that this is an artifact of either the measurement method or the extrapolation of data to zero rate of shear. It is worth noting that for PE II, the slope D is nearly constant and its value in agreement with those in Fig. 24. This may have a significant impact on the generalization of this approach. If the curves η-Y_s for samples of similar polydispersity have a similar form, then they can be scaled up by vertical shifting in a manner previously proposed (12) for n-paraffins. As a corollary - samples of different polydispersity (and branching) cannot be scaled by simple vertical shifting.

VII. PS. The data on the T and P dependence of η for polystyrene, PS, were tabulated by Cogswell and McGowan (39). To calculate Y_s, the values of F*'s were taken from the Olabisi and Simha paper (32). The assumption $P_r^* = 2\,P^*$ was used. The results are shown in Fig. 26. In the full range of T = 443 to 483 (K) and P = 0 to 140 (MPa), in which η varies within four decades of magnitude, the data follow a single "master curve". In the figure, the data of Knappe et al. (43) at T = 438 (K) and P = 0 to 145 (MPa) are also shown. Excepting the lowest η-value (ambiant P) all the other points follow the results reported by Cogswell and McGowan.

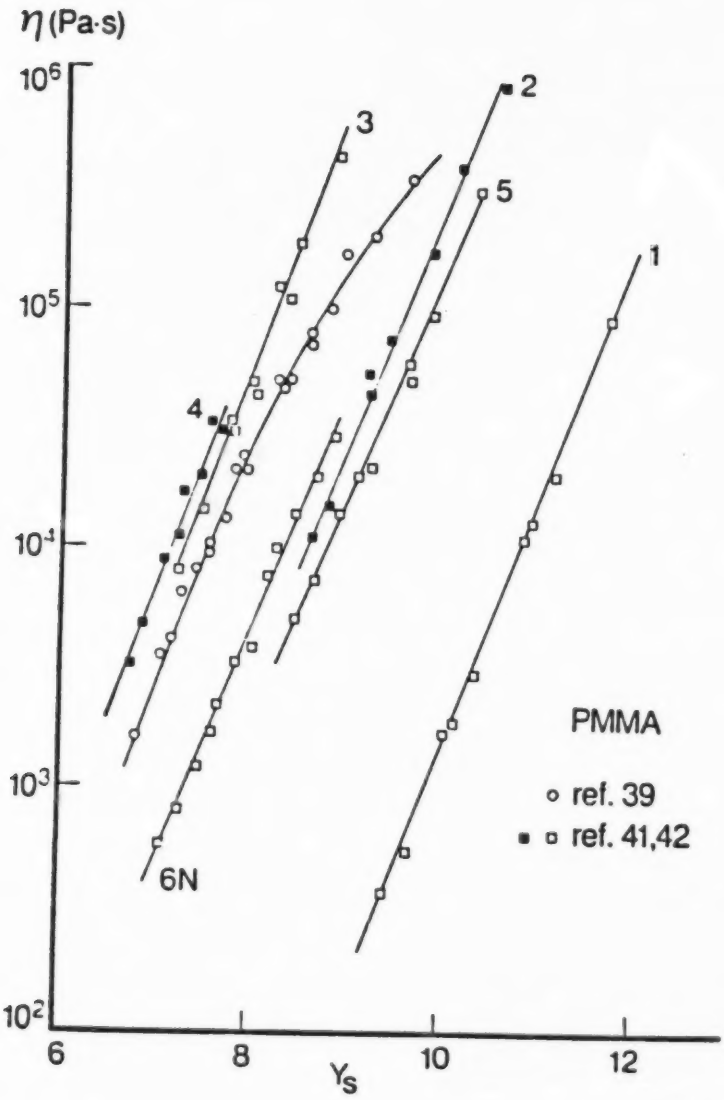

Fig. 27 $\eta - Y_s$ dependence for PMMA at T = 493 to 523 K and P ≤ 173 MPa for one sample (39) and T = 413 to 528 K and P ≤ 50 MPa for the others (41, 42). Since there were no systematic differences between different isothermal sets of data, there is no distinction of T in the Figure; the two types of points used are to distinguish dependencies of different samples.

VIII.PMMA. Viscosities of poly(methyl methacrylate), PMMA, at T = 493 to 523 (K) and P up to 173 (MPa) were reported by Cogswell and McGowan (39) and those at T = 413 to 528 and P = 5 to 50 (MPa) by Christman et al. (41, 42). To compute Y_s the F*'s were taken from Olabisi and Simha (32). The resulting plots η vs Y_s for $P_r^* = 2\ P^*$ are presented in Fig. 27.

Data from both sources are presented in the figure. For each polymer, all the results of isothermal η-P measurements followed the same "master curve". To avoid confusion there is no distinction of temperature in the Figure. In spite of overlapping ranges of Y_s for the two sources of data, those from Cogswell follow a distinct curvature, similar to the one observed for n-paraffins, while the ones from Christman give straight lines. The parameters of these lines

$$\eta = A_2 \exp \{B_2\ Y_s\} \qquad (20)$$

with the correlation coefficient squares are listed in Table 4 along with the molecular parameters (41, 42) and $\eta(Y_s = \text{constant})$.

There is no correlation between the slope B_2 and M_w/M_n. In fact, assuming the average value of B_2 for all samples: $B_3 = 2.33 \pm 0.15$ the appropriate values of A_3 listed in Table 4 can be calculated from Eq (20). It can be seen that there is no correlation between the molecular parameters M_w or M_w/M_n and A_2, A_3 or $\eta(Y_s = \text{const.})$. In particular, η's of sample 5 seems to be about two orders of magnitude too small. The origin of this discrepancy is unknown.

DISCUSSION

In Table 5 the systems analyzed in this work are listed, along with their F*'s values. Out of the eight systems two followed those previously observed for n-paraffins behaviour with $P_r^* = P^*$ (SiOil, PP), two demonstrated a transitional behaviour (PDMS, PB), in one

Table 4. Characteristics of PMMA samples (41, 42)

N°	$M_w.10^{-3}$	M_w/M_n	$A_2.10^5$	B_2	r^2	$A_3.10^5$	$\eta(Y_s=8.5)\times10^{-4}$
1	13	1.73	0.005455	2.392	0.995	0.01081	0.0039
2	48	1.78	3.0947	2.291	0.979	2.174	2.7
3	105	1.95	9.0829	2.526	0.990	44.318	21.
4	160	2.35	64.1404	2.311	0.967	56.476	26.
5	160	2.96	9.2616	2.111	0.989	1.168	1.6
6N	124	1.85	5.6734	2.277	0.993	3.758	1.4
6H	184	1.96	47.8334	2.169	0.977	13.555	7.6

case (LDPE) depending on the source of data, the results could be fitted either with $P_r^*=P^*$ or $P_r^*=2P^*$ and the remaining three systems (HDPE, PMMA and PS) obeyed the $P_r^*=2P^*$ assumption.

The error in rheological testing under ambiant pressure depends on the type of equipment and care during the measurements. Under the best circumstances ±5% accuracy is obtained while in capillary flows ±20% is considered reasonable. In the high pressure measurements a spread of data up to 70% was reported (42).

Other sources of error are the methods of extracting the zero-shear viscosities from the measured shear rate dependent function, $\eta_\dot{\gamma}$. In most of the source references the method is not provided. In the case of LDPE, HDPE and PMMA (41,42) the Spencer-Dillon (44) principle:

$$1/\eta = \lim_{\sigma_{12} \to 0} \eta_{\dot{\gamma}}^{-1} \quad , \qquad (21)$$

TABLE 5. Summary of Results

No.	System	Range of variables		Ref.	Reducing Parameters			Ref.	Superposition	
		T (K)	P (MPa)		P* (MPa)	T* (K)	$V^*.10^3$ (m^3/Kg)		P_r*/P*	depend.
1	SiOil	273-419	0- 770	29	644.4	9967	0.916	this work	1	linear
2	PDMS	298-353	0- 100	30	439	7770	0.954	"	1&2	trans.
3	PB-1	273-491	0-1000	29	767	9019	1.145	"	"	"
	PB-2	273-491	0-1000	29	713	9049	1.136	"	"	"
	PB-3	273-491	0-1000	29	767	9306	1.132	"	"	"
4	PP	487-506	0- 138	37	542	11155	1.195	38	1	curve
5	LDPE	423-543	0- 175	39	729	10620	1.167	32	2	"
	"	403-463	0- 500	40	729	10620	1.167	"	lor2	"
	"	413-493	5- 50	41,42	729	10620	1.167	"	lor2	"
6	HDPE	423-463	0- 140	39	716	10046	1.155	"	2	linear?
	"	413-493	5- 50	41,42	716	10046	1.155	"	2	curves
7	PS	443-483	0- 140	39	745	12680	0.960	"	2	linear?
8	PMMA	493-523	0- 173	39	930	11890	0.835	"	2	curve
	"	413-528	5- 50	41,42	930	11890	0.835	"	2	linear

was used (σ_{12} is the shear stress). However, this principle was shown (45) to lead to significant error; the Newtonian viscosity is reached at final (but undefined) value of $\sigma_{12,c} \neq 0$. This means that the quoted (41,42) η's are most likely too high. It is easy to see that according to Eq (21) η is defined as the true zero-shear stress (or shear rate) parameter, whereas for most systems the Newtonian plateau: $\sigma_{12} \propto \dot{\gamma}$ is found for $\sigma_{12} \leq \sigma_{12,c}$.

Another possible source of error is the computational procedure of F*'s. It is based on the assumption that Eq (5) is a good approximation of the $\tilde{V}$-$\tilde{T}$ behaviour, as predicted by the coupled Eqs (12) and (13). While Eq (5) can reproduce the exact value of V given by Eqs (12-13) to a fraction of a percent, nevertheless it is an approximation of a higher order curve. As a consequence particularly V*, determined from extrapolation of $\tilde{V}$-$\tilde{T}$ and V-T to T=0, is sentitive to the selected zone of $\tilde{T}$ used to compute S_o (viz. Eq (15)). The changes in V* are further magnified in calculating Y_s. Obviously, one should bypass Eq (5) simultaneously computing F*'s from fitting experimental data directly to Eqs (12-13). This procedure is being developed at DSM in Holland (46). The variability of P* presented in Figs. 4 and 9 is, at least partially, due to imprecise determination of V* and T*.

The difficulties in determination of η as well as those in computation of F*'s do not explain why it is that for most polymers the rheological P_r^* is about twice as large as P*. It should be mentioned that from superposition of the pressure dependent dynamic-mechnical data for four rubbers Moonan and Tschoegl (47) found $P_r^*/P^* = 1.29$ to 2.23.

In PS, PMMA and HDPE, where $P_r^* = 2P^*$, there is either "more" free volume available for flow or there is a "more economical" way to utilize the available volume. The theory predicts that (28):

$$P^*V^*/T^* = R/3M_o \qquad (22)$$

where R is the gas constant and M_o is the molecular weight of the statistical segment defined as: $M = sM_o$, where M is the molecular weight of the polymeric molecule. Increasing P* by a factor of two indicates that in flow, the effective segment length is about one-half of that observed in thermodynamics. From Table I of (32), one can write:

$$M_o = 4.6868.10^{-3}\ T^* - 12.5876\ ; \qquad r^2=0.948, \qquad (23)$$

i.e. thermodynamically the lattice cell volume (proportional to M_o) increases linearly with T* at T* varying from 5880 to 12740 K. Alternatively the data for n-paraffins (25,26) can be presented as:

$$M_o = 33.278/[1+6.5265/n]; \qquad r^2 = 0.9979, \qquad (24)$$

where n is the number of C in n-paraffin chain. For $n \to \infty$, i.e. for HDPE, M_o=33.278 to be compared with the experimental values: 31.7 to 33.7. In short, the P-V-T results indicate a systematic increase of cell volume with the size of the molecule.

It is interesting to note that the requirement: $P_r^* = 2P^*$ is equivalent to reduction of cell volume by a factor of two, i.e. reduction of M_o to about 16-17, characteristic of C_6 to C_7. If the flow occurs by coordinated segmental jumps, one may expect that in a homologous series the size of the segment (for molecules above a certain size) will be relatively independent of the total molecular weight. It seems that the analysis provided in this paper indicate this to be the case.

In some systems (PDMS, PB) a transition has been observed. The pressure at which the transition occurs increased with T. The plot of these P_{cr}-T_{cr} pairs is a sort of phase diagram for transition in flow, equivalent to a standard V-T diagram. In the area of higher T and lower P (or higher V) $P_r^*=P^*$ is obeyed, on the other side of the curve $P_r^*=2P^*$. It should be noted that the factor

of 2 is not the optimal value required for superposition of η - Y_s data on a single curve; in this work, the factor was chosen arbitrarily to facilitate the procedure. This is only justified only by previous computation of data (15) in which 2.0 ± 0.2 was found for PS and PMMA.

In Fig. 21 η vs M_w plot is shown. The data follow relatively well (r^2=0.950) Eq (15). Since the extrapolation method to obtain the Newtonian η is suspect, the relation should be compared with other reported results. The recent data (48):

$$\eta_o = 2.692 \cdot 10^{-14} M_w^{3.49} \quad ; \quad r^2 = 0.996 \qquad (25)$$

compared fairly well with Eq (18). As expected Chritmann's data are higher by a factor of 1.8 at the lower, and by 1.4 at the higher end of the M_w range. This, relatively constant variation may be due to the pressure effect (P = 5 MPa data were used) and it should not influence the validity of conclusions drawn from η - Y_s dependencies for these resins.

CONCLUSIONS

The zero-shear viscosity of liquids can be written as a unique function of the free volume, f:

$$\ln \eta = A_4 + A_5/(f+A_6) \qquad (26)$$

where A_i are parameters and f is the effective free volume: $f=f(T/T^*, P/P_r^*)$. For low-viscosity liquids: $P_r^* = P^*$, for high-η ones: $P_r^* = 2P^*$. To calculate $\eta(P)$ at T=const. one should determine $\eta = y(T)$ in as wide a range of T as possible. Using $P_r^* = 2P^*$ such a dependence can be cast into a form of Eq (26) in which f is accessible from statistical thermodynamics.

The above recommendation is valid within the full range of independent variables only for liquids of the same structure. In systems undergoing phase transition (crystallization or liquid-liquid type) the treatment has to be different for each phase; usually superposition of the lower-η phase can be accomplished using $P_r^*=P^*$, whereas that of the higher-η one using $P_r^* = 2P^*$.

It is highly advisable to develop a simultaneous fit of P-V-T data to Eqs (12-13). Such a method, bypassing the empirical Eq (5), will lead to improved precision in determination of F*'s. This improvement is needed to achieve desired accuracy in computation of f.

Finally, the need for $\eta(P,T)$ data for polymeric liquids must be stressed. Even within the low pressure range observed during extrusion: $P < 50$ MPa these are difficult . The data in the higher range, $P < 700$ MPa, experienced in injection molding, are virtually non-existent (see Table 5). The analysis of existing $\eta(P,T)$ data of oligomeric and polymeric liquids demonstrates the complexity of the problem. The complexity is a consequence and

extension of the behaviour observed previously under the ambiant pressure (7-9). It would be unrealistic to expect $\eta = \eta(P)$ to be simpler than $\eta = \eta(T)$. In both cases the liquid-liquid or liquid-solid transitions have to be watched for. However, within a single phase (structure) the $\eta(P,T)$ dependence can be predicted.

One particularly interesting conclusion of this work is that in a homologous series of liquids, i.e. in a series of liquids with variable molecular weight (viz. n-paraffins, HDPE of constant polydispersity) it is possible to generate a master curve for the whole series. In this case Eq (26) can be expressed as:

$$\ln\eta/\eta^* = A_5(f^*-f)/(f+A_6)(f^*+A_6) \qquad (27)$$

where η^* is the viscosity at an arbitrarily selected value of f^*. Eq (27) has a particularly simple form in cases where $A_6 = 0$, as for SiOil, HDPE, PS and PMMA and for PDMS and PB at $P \gtrless P_{cr}$.

ACKNOWLEDGEMENTS

In preparation of this manuscript the author profited greatly prefined from numerous discussions with Profs. R. Simha, M. Grmela, N.W. Tschoegl and R. Koningsveld. The thesis of Dr. L. Christmann was received through the courtesy of Prof. W. Knappe. Thank you very much.

REFERENCES

1. NRCC-IMRI mini-symposium series on mathematical modeling of plastics processing and properties: "Modeling-'82" held February 9th, 1982, published in Polymer Eng. Sci., 22(17), (1982); "Modeling-'83", held February, 1983, published in Polymer Eng. Sci., 24( ), (1984).

2. P. Avenas, J.F. Agassant et J.Ph. Sergent, "La mise en forme des matières plastiques", T & D. Lavoisière, Paris, 1982.

3. J.R.A. Pearson and S.M. Richardson, Eds., "Computational analysis of polymer processing", Applied Science, London, 1983.

4. F.N. Cogswell, "Polymer Melt Rheology", G. Godwin Ltd., London, 1981.

5. A.B. Metzner in "Processing of Thermoplastics Materials", E.C. Bernhardt, Ed., R.E. Krieger Publ. Co., Malabar, FA, 1959, Section I.

6. L.A. Utracki, Polymer Eng. Sci., 23, 446 (1983).

7. L.A. Utracki, J. Macromol. Sci., Phys., B10, 447 (1974).

8. L.A. Utracki, J. Macromol. Sci., Phys., B18, 731 (1980).

9. L.A. Utracki and R. Simha, J. Rheol., 25, 329 (1981).

10. L.A. Utracki, Polymer Eng. Sci., 22, 81 (1981).

11. L.A. Utracki and R. Simha, A.C.S. Polymer Prepr., 23 (2), 67 (1982).

12. L.A. Utracki, Canad. J.Chem. Eng., 61, 753 (1983).

13. R. Simha and C.E. Weil, J. Macromol. Sci. - Phys. B4, 215 (1970).

14. A.J. Batschinski, Z. Phys. Chem., 84, 643 (1913).

15. L.A. Utracki, A.C.S. Polymer Prepr., 24(2), 113 (1983).

16. R. Simha and T. Somcynski, Macromolecules, 2, 342 (1969).

17. J.E. McKinney and R. Simha, Macromolecules, 9, 430 (1976).

18. R. Simha, Makromol. Chem. Suppl., 2, 143 (1979).

19. R.K. Jain and R. Simha, J. Chem. Phys., 72, 4909, (1980).

20. R.K. Jain and R. Simha, Macromolecules, 13, 1501 (1980).

21. R.K. Jain, R. Simha and P. Zoller, J. Polym. Sci., Polymer Phys. Ed., 20, 1399 (1982).

22. R. Simha, Macromolecules, 10, 1025 (1977).

23. R.K. Jain and R. Simha, Berichte Bunsen Gess. Phys. Chem., 85, 626 (1981).

24. O. Olabisi and R. Simha, Macromolecules, 8, 211 (1975).

25. R.K. Jain and R. Simha, J. Chem. Phys., 85, 2182 (1981).

26. R.K. Jain and R. Simha, J. Chem. Phys., 70, 5329 (1979).

27. J.G. Curro, R.R. Lagasse and R. Simha, Paper presented at Phoenix meeting of the A.P.S., March 16-18, 1981, see also J. Appl. Phys. 52, 5892 (1981); Macromolecules, 15, 1621 (1982).

28. R. Simha, Polymer Eng. Sci., 22, 74 (1982).

29. American Society of Mechanical Engineers, "Viscosity and Density of over 40 Lubricating Fluids of Known Composition at Pressures to 150,000 PSI and Temperature to 425°F", Research Report on Pressure Viscosity, Vols I and II (1953).

30. S. Tokiura, S. Ogihara, T. Takaki and H. Sasaki, "Proceedings Intl. Congress Rheolog. Tokyo 1968", S. Onogi (Ed.), Tokyo Press pg. 275 (1970).

31. P.G. Tait, "Report on some of the physical properties of fresh water and sea water" in Rept. Sci. Results Voyage H.M.S. Challenger, Phys. Chem. 2, 1-76 (1888).

32. O. Olabisi and R. Simha, J. Appl. Phys., 21, 149 (1977).

33. W.A. Lee, J. Polymer Sci., A-2, 8, 555 (1970).

34. R.F. Boyer, Macromolecules, 7, 142 (1974).

35. R.F. Boyer, J. Macromol. Sci, Phys., B18, 455 (1980).

36. R.F. Boyer, Colloid Polym. Sci., 258, 760 (1980).

37. R.G. Foltz and K.K. Wang, J. Non-Newtonian Fluid Mech., 3, 347 (1978).

38. P.J. Zoller, J. Polymer Sci., Polym. Phys. Ed., 16, 1491 (1978).

39. F.N. Cogswell and J.C. McGowan, Br. Polymer J., 4, 183 (1972).

40. V.-H. Karl, Ang. Makromol. Chem., 79, 11 (1979).

41. L. Christmann and W. Knappe, Colloid Polymer Sci., 252, 705 (1974).

42. L. Christmann, Dr. rer. nat. - Thesis, Technischen Hoschschule Darmstadt, 1977.

43. K. Helwege, W. Knappe, P. Paul and V. Semjonow, Rheol. Acta, 6, 165 (1967).

44. R.S. Spencer and R.E. Dillon, J. Colloid Sci., 3, 163 (1948); ibid, 4, 241 (1949).

45. K.K. Chee and A. Rudin, Can. J. Chem. Eng., 48, 362 (1970).

46. R. Koningsveld, private communication.

47. N.W. Tschoegl, private communication.

48. J.Y. Decrox and M. Hert, 5^{e} Conf. Europ. Plast. - Caoutchouc, 1978, Proceedings, Paper N° E-9.

POOR

QUALITY

ORIGINAL